Hubble Space Telescope Spectroscopy of Spot 1 on the Circumstellar Ring of SN 1987A

THE ASTROPHYSICAL JOURNAL, 542:L53–L56, 2000 October 10

HUBBLE SPACE TELESCOPE SPECTROSCOPY OF SPOT 1 ON THE CIRCUMSTELLAR RING OF SN 1987A

ELI MICHAEL,[1] RICHARD MCCRAY,[1] C. S. J. PUN,[2] PETER GARNAVICH,[3] PETER CHALLIS,[3] ROBERT P. KIRSHNER,[3] JOHN RAYMOND,[3] KAZIMIERZ BORKOWSKI,[4] ROGER CHEVALIER,[5] ALEXEI V. FILIPPENKO,[6] CLAES FRANSSON,[7] PETER LUNDQVIST,[7] NINO PANAGIA,[8] M. M. PHILLIPS,[9] GEORGE SONNEBORN,[2] NICHOLAS B. SUNTZEFF,[10] LIFAN WANG,[11] AND J. CRAIG WHEELER[11]

Received 1999 September 10; accepted 2000 August 10; published 2000 September 19

ABSTRACT

We present ultraviolet and optical spectra of the first bright spot (P.A. = 29°) on SN 1987A's equatorial circumstellar ring taken with the Space Telescope Imaging Spectrograph. We interpret this spot as the emission produced by radiative shocks that occur where the supernova blast wave strikes an inward protrusion of the ring. The observed line widths and intensity ratios indicate the presence of radiative shocks with velocities ranging from 100 to 250 km s^{-1} entering dense ($\gtrsim 10^4$ cm^{-3}) gas. These observations, and future observations of the development of the spectra and line profiles, provide a unique opportunity to study the hydrodynamics of radiative shocks.

Subject headings: circumstellar matter — shock waves — supernova remnants — supernovae: individual (SN 1987A)

1. INTRODUCTION

After the discovery of the circumstellar ring around SN 1987A, several authors pointed out that the supernova blast wave should strike the ring some 10–20 yr after the supernova explosion (Luo & McCray 1991; Luo, McCray, & Slavin 1994; Chevalier & Dwarkadas 1995; Borkowski, Blondin, & McCray 1997b). The estimated time of first contact was uncertain, mainly because it depended on the unknown density of circumstellar gas between the supernova and the ring.

This event is now underway. In 1997 an unresolved brightening spot was detected at position angle ~29° (spot 1) on the near (north) side of the ring (Pun et al. 1997; Garnavich, Kirshner, & Challis 1997). Lawrence et al. (2000) trace the appearance of this spot back to 1995. This spot continues to brighten, and within the last year several new spots have appeared (Lawrence & Crotts 2000; Garnavich, Kirshner, & Challis 2000; Lawrence et al. 2000). A shock interpretation for these spots was suggested by Space Telescope Imaging Spectrograph (STIS) observations of the ring taken in 1997 (Sonneborn et al. 1998). The spectral image of the ring in Hα showed a streak at the position of spot 1, indicating blueshifted emission with velocities up to ~250 km s^{-1}. Evidently, at the positions of the spots, the blast wave is striking inward protrusions of the dense equatorial ring.

In § 2 we report on early optical and ultraviolet STIS spectra of SNR 1987A, which show several broad lines associated with spot 1. In § 3 we present the radiative shock model for the emission from the spots, and in § 4 we discuss what we can infer from the spectrum and its evolution.

2. OBSERVATIONS

The Supernova Intensive Study collaboration obtained STIS spectra of spot 1 at ultraviolet and optical wavelengths in 1997 September and 1998 March, respectively. The ultraviolet spectrum (not shown) was taken on 1997 September 27 (3869.3 days since the explosion) with the G140L low-dispersion grating (1150–1736 Å, $\Delta v \approx 300$ km s^{-1}) and a 0.″5 slit. Five spectral images totaling 11,200 s were combined. Emission lines from nearly stationary gas in the ring are apparent at N v λλ1239, 1243, O IV] λ1400, N IV] λ1487, and He II λ1640. Emission from spot 1 is also visible in these lines, as well as Si IV λλ1394, 1403, [N IV] λ1483, and C IV λλ1548, 1551. The low-velocity Si IV and C IV emission from the ring is blocked by interstellar absorption (Fransson et al. 1989). As a result of geocoronal Lyα emission, no information about Lyα from the spot was obtained.

The optical spectrum was taken on 1998 March 7 (4030.0 days since explosion) with a 0.″2 slit and the G750M grating (6295–6867 Å, $\Delta v \approx 50$ km s^{-1}). Three spectral images totaling 8056 s were combined. A section of the optical spectrum is shown in Figure 1. The central horizontal streak (which extends to $\sim \pm 3000$ km s^{-1}) is Hα emission from the radioactively heated supernova debris. Pairs of bright spots where the slit intersects the stationary inner ring are evident in [N II] λλ6548, 6584 and Hα (not displayed but also present are [O I] λλ6300, 6364, He I λ6678, and [S II] λλ6717, 6731). Three fainter spots due to the outer rings are also visible in Hα and [N II]. Broad streaks of emission from spot 1 appear on the upper segments

[1] Joint Institute for Laboratory Astrophysics, University of Colorado, Boulder, CO 80309-0440; michaele@colorado.edu.
[2] NASA Goddard Space Flight Center, Laboratory for Astronomy and Space Physics, Code 681, Greenbelt, MD 20771.
[3] Harvard-Smithsonian Center for Astrophysics, 60 Garden Street, Cambridge, MA 02138.
[4] Department of Physics, North Carolina State University, Raleigh, NC 27695.
[5] Department of Astronomy, University of Virginia, P.O. Box 3818, Charlottesville, VA 22903-0818.
[6] Department of Astronomy, University of California, Berkeley, Berkeley, CA 94720-3411.
[7] Stockholm Observatory, SE-133 36 Saltsjöbaden, Sweden.
[8] Space Telescope Science Institute, 3700 San Martin Drive, Baltimore, MD 21218; on assignment from the Space Science Department of ESA.
[9] Las Campanas Observatory, Carnegie Observatories, Casilla 601, La Serena, Chile.
[10] Cerro Tololo Inter-American Observatory, NOAO, Casilla 603, La Serena, Chile.
[11] Department of Astronomy, University of Texas, Austin, TX 78712.

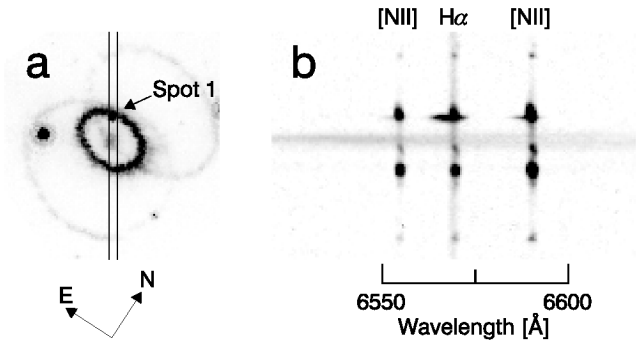

FIG. 1.—(*a*) Slit orientation on image of SN 1987A's triple-ring system. (*b*) Section of STIS G750M optical spectrum (the intensity scale has been stretched to show the hot spot emission).

of the ring lines. These streaks are inside the ring emission indicating that spot 1 lies at the inner edge of the ring.

The spectra of spot 1 are extracted from the STIS spectral images. For the optical emission lines, the major source of contamination is the emission from the nearly stationary ($v = 10.5 \pm 0.3$ km s^{-1}; Crotts & Heathcote 2000) circumstellar ring filling the 0.″2 (≈100 km s^{-1}) slit. The Hα line profile is shown in Figure 2. The parts of the line profiles that lie outside of the ring emission are fit well by Gaussians. The velocity shifts of the Gaussian fits are poorly constrained since the spot's spatial position in the slit is uncertain. In the ultraviolet, the ring emission is much weaker, and therefore its contribution to the extracted spot 1 spectrum is neglected. The UV lines are poorly resolved at the resolution of the G140L grating. It is possible to account for the detector line-spread function in order to obtain intrinsic widths for the UV lines (C. S. J. Pun et al. 2000, in preparation). While this method introduces errors in the determined width, we find that all the UV lines have intrinsic widths less than 400 km s^{-1}.

All the lines from spot 1 were fit with Gaussians in order to extract their fluxes and FWHMs (see Table 1). The errors stated in Table 1 are 1 σ statistical errors to the fits. Close multiplets (N v λλ1239, 1243 and C iv λλ1548, 1551) were fit simultaneously by requiring a set wavelength separation, identical widths, and line ratios dictated by their oscillator strengths. For the N v doublet, the emission from spot 1 overlapped with very broad Lyα emission (∼ ± 15,000 km s^{-1}) from

TABLE 1

EMISSION LINES FROM SPOT 1

Emission Line	FWHM (km s^{-1})	Observed Flux ($\times 10^{-16}$ ergs cm^{-2} s^{-1})
N v λλ1239, 1243	...	2.5 ± 0.9
Si iv λλ1394, 1403	...	0.6 ± 0.2
O iv] λ1400	...	1.3 ± 0.4
[N iv] λ1483	...	1.4 ± 0.4
N iv] λ1487	...	1.5 ± 0.4
C iv λλ1548, 1551	...	2.9 ± 0.8
He ii λ1640	...	3.5 ± 0.9
[O i] λ6300	154 ± 7	8.9 ± 0.7
[O i] λ6364	179 ± 14	3.3 ± 0.4
[N ii] λ6548	165 ± 11	5.6 ± 0.8
Hα λ6563	253 ± 4	46.7 ± 1.2
[N ii] λ6584	204 ± 7	13.1 ± 0.9
He i λ6678	177 ± 38	0.8 ± 0.2
[S ii] λ6717	113 ± 40	0.9 ± 0.9
[S ii] λ6731	149 ± 48	0.9 ± 0.4

the reverse shock (Sonneborn et al. 1998; Michael et al. 1998). This Lyα background was removed using a quadratic fit and is the source of the large uncertainty in the N v λλ1239, 1243 flux. At the G140L resolution, the Si iv λ1403 emission of spot 1 is mixed with that from the O iv] λ1400 multiplet. Using the measured Si iv λ1394 flux and assuming $I(1394)/I(1403) = 2$, the Si iv λ1403 flux was determined and removed from the O iv] λ1400 multiplet.

In addition to interstellar extinction, the observed C iv and Si iv fluxes are further reduced by line absorption along the line of sight to the supernova. The absorption profiles for these lines are known from *IUE* high-dispersion spectra of SN 1987A taken at the time of outburst (Welty et al. 1999). Since the intrinsic profiles of the lines are poorly known, correcting for this absorption is a somewhat uncertain endeavor. For now we present just the observed fluxes and note that under reasonable assumptions of the intrinsic profiles we find correction factors of ≈2 for these lines (C. S. J. Pun et al. 2000, in preparation).

3. RADIATIVE SHOCK MODEL

Figure 3 illustrates the scenario that we believe accounts for the emission from spot 1. The freely expanding supernova ejecta are slowed from ∼15,000 to ∼4000 km s^{-1} by a reverse shock. The shocked gas drives a blast wave (forward shock), with velocity $v_b \approx 4000$ km s^{-1}, into an H ii region having density $n_{\rm H\,II} \approx 100$ cm^{-3} (Chevalier & Dwarkadas 1995; Borkowski,

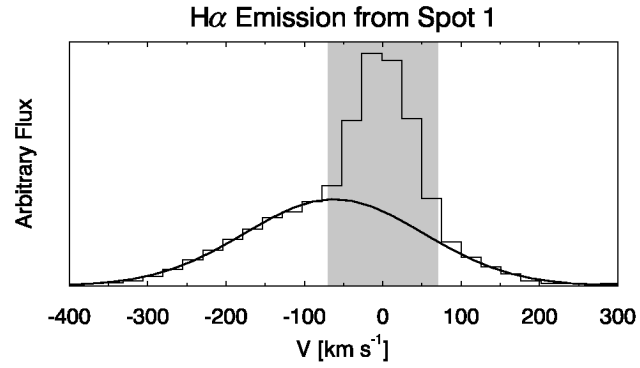

FIG. 2.—Hα profile of spot 1 extracted from the G750M spectrum. Low-velocity emission (*shaded region*) from unshocked stationary ring material defines the standard of rest. A Gaussian fit to the broad emission from shocked gas is shown.

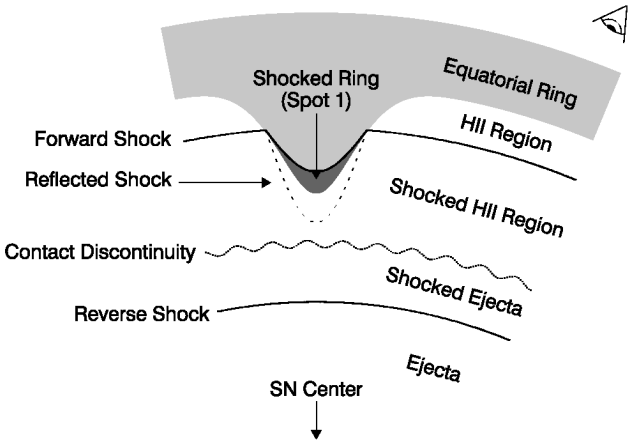

FIG. 3.—Cartoon of SNR 1987A's structure in the equatorial plane

Blondin, & McCray 1997a; Lundqvist 1999). The bright spots occur where the blast wave encounters protrusions of the dense ($n \approx 10^4$ cm^{-3}; Lundqvist & Fransson 1996) equatorial ring. As it enters a protrusion, the blast wave is slowed to a value $v_s \approx v_b(n_{\rm H\,II}/n)^{1/2} f(\theta)$, where θ is the angle between the surface of the protrusion and the propagation direction of the blast wave. The function $f(\theta)$, which accounts for shock obliquity and the pressure increase due to the reflected shock, varies from $f(0) \approx 2$ at the head of the protrusion to $f(\pi/2) \approx 0.7$ along its sides (Borkowski et al. 1997b). We therefore expect a range of shock velocities, $280 n_4^{-1/2}$ km s$^{-1} \lesssim v_s \lesssim 800 n_4^{-1/2}$ km s^{-1}, to be present (where n_4 is the preshock density in units of 10^4 cm^{-3}).

An important parameter for the shocks considered here is the radiative cooling time t_c, defined as the time for the shocked gas to cool from the postshock temperature, $T_s = 3\ \mu {\rm m}_p v_s^2/16k \approx 1.2 \times 10^6\ (v_s/300\ {\rm km\ s^{-1}})^2$ K, to $T_c = 10^4$ K. A fit to the results from a plane-parallel steady state shock code (e.g., Cox & Raymond 1985) with abundances appropriate to SN 1987A (Lundqvist & Fransson 1996; Russell & Dopita 1992) shows that, for 100 km s$^{-1} < v_s < 600$ km s^{-1}, $t_c \approx 4.6 n_4^{-1} (v_s/300\ {\rm km\ s^{-1}})^{3.7}$ yr.

When these spectra were taken, the age of the spot, $t_{\rm spot} \approx 3$ yr, was comparable to the cooling time for shocks with the range of densities and velocities expected in the protrusion. Shocks with velocities $\gtrsim 250 n_4^{0.27}$ km s^{-1} have $t_c > t_{\rm spot}$ and will not yet have radiated away their energy, while slower (radiative) shocks will have had time to cool and will convert all their thermal energy into radiation. Nonradiative shocks produce far less ultraviolet and optical emission than radiative shocks. Therefore, although faster shocks might be present, we expect the ultraviolet and optical emission from spot 1 to be dominated by shocks with speeds $\lesssim 250 n_4^{0.27}$ km s^{-1}.

The radiative shock model does predict the presence of both strong UV and optical lines. The ultraviolet lines produced in a radiative shock come mainly from the cooling region, where the shocked gas's thermal energy is radiated away. The optical lines, however, are formed in the cool layer of dense ($\sim n T_s/T_c$, where $T_c \approx 10^4$ K) gas, which forms behind the cooling region. This photoabsorption layer quickly becomes thick enough to absorb the downstream ionizing radiation produced in the cooling region and converts the flux into optical emission lines.

The optical lines are formed with thermal widths characteristic of 10^4 K gas. The actual profiles are much broader and must be due to the macroscopic motion of fluid parcels in the photoabsorption layer. In a steady shock, the gas in the photoionization zone will have the same velocity as the shock front, and therefore the optical lines would be expected to have velocity profiles representative of the hydrodynamics of the shock (specifically, those parts of the shock that have developed a radiative layer). The presence of both redshifted and blueshifted emission can be explained by shocks traveling both into and out of our line of sight (see Fig. 3).

4. DISCUSSION

It will not be an easy task to develop a quantitative model for the spectrum and line profiles of the hot spot. As Figure 3 illustrates, these result from a superposition of shocks having a range of velocities and aspect angles that depend on the unknown geometry and density structure of the protrusion. Our task is further complicated by the fact that radiative shocks are subject to violent thermal and dynamical instabilities (e.g., Innes, Giddings, & Falle 1987; Klein, McKee, & Colella 1994; Walder & Folini 1996, 1998), so steady shock models may be inadequate to interpret the spectrum.

Despite the complexity of the actual situation, we can gain some insight into the physical conditions in the spot by comparing the actual spectra with the results from the plane-parallel steady state shock code. For example, the code shows that the ratios of the flux of N V λλ1239, 1243 to the flux of lines from lower ionization states (O IV] λ1400, N IV] λ1487, and C IV λλ1548, 1551) are sensitive functions of shock velocity. N V is not produced at temperatures $T_s \lesssim 2 \times 10^5$ K ($v_s \lesssim 120$ km s^{-1}), above which its emissivity rises rapidly with shock velocity. On the other hand, O IV, N IV, and C IV all form at lower temperatures, and their emissivities are less sensitive to velocity. To reproduce the observed ratios with the shock code we must constrain the shock velocity to the range 120 km s$^{-1} < v_s < 150$ km s^{-1}. But such a velocity range conflicts with the observed optical line widths, which require radiative shocks with velocities up to at least ≈250 km s^{-1}.

However, only ≈20% of the emission in the broad Hα line profile comes at high velocity ($|v| > 135$ km s^{-1}, measured from line center). We may then argue that only ≈20% of the Hα emission must come from shocks faster than 135 km s^{-1}. If this is true, the line ratios will be dominated by emission from the slower shocks. We find that if the slower shocks ($v_s < 135$ km s^{-1}) cover about 4 times the surface area of the faster shocks ($v_s > 135$ km s^{-1}), then the net emission from these shocks produce ratios near those observed.

The presence of both fast and slow radiative shocks indicates that the protrusion must have a slightly higher density than the average ring density. Using hydrodynamical arguments presented in § 3 we find that preshock densities $n \gtrsim 4 \times 10^4$ cm^{-3} are required to produce shocks as slow as 135 km s^{-1}. A less stringent lower limit is provided by an independent argument based on the radiative cooling time. Preshock densities of $n \gtrsim 10^4$ cm^{-3} are required for shocks as fast as 250 km s^{-1} (as indicated by the Hα line width) to cool within $t_s \approx 3$ yr.

We can also use the spectroscopic data to estimate the surface area of the shock interaction. Most of the emission comes from shocks with velocities ≈135 km s^{-1}, for which the shock code gives an Hα surface emissivity of $0.4 n_4$ ergs cm^{-2} s^{-1}. Correcting the observed Hα flux for reddening (Scuderi et al. 1996) and assuming a distance of 50 kpc, we find that the shock must have an Hα-emitting surface area of $A_s \approx 10^{33}$ cm^2 (assuming $n = 4 \times 10^4$ cm^{-3}). Then, assuming a hemispherical shape for the emitting surface, we estimate that spot 1 should have a characteristic dimension $D_{\rm spot} \approx (2A_s/\pi)^{1/2} \approx 3 \times 10^{16}$ cm (or ≈0.″04). This is smaller than *Hubble Space Telescope*'s resolution, so we are not surprised that the spot is spatially unresolved.

As Table 1 indicates, different emission lines have different widths. This is expected, since the emissivities of the lines are sensitive functions of shock velocities and a range of shock velocities is clearly in evidence. Moreover, the differences among the optical line widths may be explained by partial cooling in fast shocks. Emission from ions like O I and S II comes from regions downstream of the gas that produces Hα emission. Faster shocks take longer to develop these downstream regions. The fastest shocks that produce Hα will not yet have developed their [O I]– and [S II]–emitting zones. Therefore, the [O I] and [S II] lines are narrower than the Hα line.

Now that several new bright spots have appeared on the circumstellar ring of SN 1987A (Lawrence & Crotts 2000; Garnavich et al. 2000; Lawrence et al. 2000), we have new opportunities to elucidate the development of radiative shocks. By

observing the spectra of each of the spots, we can follow the development of shocks having different ages and velocities. The spots will continue to brighten, and their spectra will change. The pressure that drives the shocks will increase, the shocks will engulf more of the protrusions, and faster shocks will develop radiative layers. The most powerful constraint on the hydrodynamics will be resolving the line ratios as a function of Doppler velocity. For example, the wings of the N v λλ1239, 1243 line profile should be more prominent than those of C iv λλ1548, 1551. As the optical lines brighten, their wings should broaden.

For these reasons, it is imperative to observe the development of the spectra of these spots on a regular basis. These observations will need to be performed by STIS in order to obtain UV line profiles as well as spatially distinguish the spectra of the different spots.

E. M. thanks S. Zhekov for fruitful discussions. This research was supported by NASA through grants NAG5-3313 and NTG5-80 to the University of Colorado and grants GO-2563 and GO-7434 from the Space Telescope Science Institute, which is operated by the Association of Universities for Research in Astronomy, Inc., under NASA contract NAS5-26555. C. S. J. P. acknowledges support by the STIS IDT through NOAO by NASA.

REFERENCES

Borkowski, K., Blondin, J., & McCray, R. 1997a, ApJ, 476, L31
———. 1997b, ApJ, 477, 281
Chevalier, R. A., & Dwarkadas, V. V. 1995, ApJ, 452, L45
Cox, D. P., & Raymond, J. C. 1985, ApJ, 298, 651
Crotts, A. P. S., & Heathcote, S. R. 2000, ApJ, 528, 426
Fransson, C., et al. 1989, ApJ, 336, 429
Garnavich, P., Kirshner, R., & Challis, P. 1997, IAU Circ. 6710
———. 2000, IAU Circ. 7360
Innes, D. E., Giddings, J. R., & Falle, S. A. E. G. 1987, MNRAS, 226, 67
Klein, R. I., McKee, C. F., & Colella, P. 1994, ApJ, 420, 213
Lawrence, S. S., & Crotts, A. P. S. 2000, IAU Circ. 7359
Lawrence, S. S., et al. 2000, ApJ, 537, L123
Lou, D., & McCray, R. 1991, ApJ, 379, 659
Lou, D., McCray, R., & Slavin, J. 1994, ApJ, 430, 264
Lundqvist, P. 1999, ApJ, 511, 389
Lundqvist, P., & Fransson, C. 1996, ApJ, 464, 924
Michael, E., et al. 1998, ApJ, 509, L117
Pun, C. S. J., et al. 1997, IAU Circ. 6665
Russell, S. C., & Dopita, M. A. 1992, ApJ, 384, 508
Scuderi, S., et al. 1996, ApJ, 465, 956
Sonneborn, G., et al. 1998, ApJ, 492, L139
Walder, R., & Folini, D. 1996, A&A, 315, 265
———. 1998, A&A, 330, L21
Welty, D. E., Frisch, P. C., Sonneborn, G., & York, D. G. 1999, ApJ, 512, 636